

PAPER • OPEN ACCESS

## Comparison Between Performance of De-ionized Water and Al<sub>2</sub>O<sub>3</sub>/De-ionized Water on Enhancing the Transportation of Heat in Small Space

To cite this article: Nazih A Bin-Abdun *et al* 2019 *IOP Conf. Ser.: Mater. Sci. Eng.* **557** 012051

View the [article online](#) for updates and enhancements.

# Comparison Between Performance of De-ionized Water and Al<sub>2</sub>O<sub>3</sub>/De-ionized Water on Enhancing the Transportation of Heat in Small Space

Nazih A Bin-Abdun<sup>1,2</sup>, Z M Razlan<sup>1,\*</sup>, S A Bakar<sup>1</sup>, C H Voon<sup>3</sup>, W K Wan<sup>1</sup>, I Zunaidi<sup>4</sup>, M K Albzeirat<sup>5</sup> and N Z Noriman<sup>6</sup>

<sup>1</sup>School of Mechatronic Engineering, Universiti Malaysia Perlis, Pau Putra Campus, 02600 Arau, Perlis, Malaysia

<sup>2</sup>Seiyun Community College, Department Air-Conditioning, Hadhramoot, Yemen

<sup>3</sup>Institute of Nano Electronic Engineering, University Malaysia Perlis, Seriab, 01000, Kangar, Perlis, Malaysia

<sup>4</sup>Faculty of Technology, University of Sunderland, St Peter's Campus, Sunderland, SR6 0DD, United Kingdom

<sup>5</sup>School of Manufacturing Engineering, University Malaysia Perlis, Pau Putra Campus, 02600 Arau, Perlis, Malaysia

<sup>6</sup>Faculty of Engineering Technology, Universiti Malaysia Perlis, UniCITI Alam Campus, Sungai Chuchuh, 02100 Padang Besar, Perlis, Malaysia

<sup>a</sup> Corresponding author: zuradzman@unimap.edu.my

**Abstract.** In this article, the influence of deionized water and Al<sub>2</sub>O<sub>3</sub>/deionized water nanofluid to cooling battery ambient temperature is shown in figure 1. The battery temperature is observed to be decrease as the Al<sub>2</sub>O<sub>3</sub>/deionized water nanofluids volume concentration and high flow rate is incremented. The Al<sub>2</sub>O<sub>3</sub>/deionized water nanofluid exhibits enhancement as compared to deionized water under laminar flow conditions. The 0.60 vol. % concentration of Al<sub>2</sub>O<sub>3</sub> with 10g surfactant and 1 L/min flow rate gives the highest heat transfer rate value among all with 65 % higher as compared to deionized water at laminar flow was observed. It has been observed that 24 hr of ultra-sonication was the best duration in the presence of a surfactant, where it gives the best stability and improved thermal conductivity, this improvement is due to decrease of aggregates within nanoparticle.

## 1. Introduction

Transportation of heat is one of the significant manufacturing processes [1]. Long-established heat transfer fluids such as oil engine, ethylene glycol, pure water, etc, have not given enough enhancement for cooling systems because of their comparatively low thermal conductivity [2], [3]. Thence, the development of highly efficient working fluids is disbanding the disadvantages of conventional fluids has become one of the most significant priorities in the cooling systems. It was determined in the literature review that using nanofluids instead conventional fluids enhances the transportation of heat by incrementing the thermal conductivity of the nanofluid compared to the conventional fluids [4].



## 2. Experimental Apparatus

Figure 1 shows the experimental preparation diagram for measuring the heat transfer performance. The experimental devices employed involves fluid flow pipes, DC pump (Max. Flow: 9 L/Min), a flowmeter (1.2 L/Min), a stainless steel tank used of fluids ( $\text{Al}_2\text{O}_3$ / deionized water or deionized water) storage (1 litre), two-Temperature Bath (one to control the fluid temperature (cooler, 20 °C), and another is for controlling the water temperature (heater, 40 °C), which represents heat load of battery, heat exchanger made from copper coils (two coils, length every one equal 2.2 m), ten-thermocouples (K-type, accuracy equal  $\pm 0.1$  °C ) are installed on experiment parts (represented by red dots). The fluid was pumped to the heat exchanger in the test compartment (battery compartment) from a stainless-steel tank that the temperature was controlled by the temperature bath (cooler). A water that the temperature was being controlled from the temperature bath (heater) was pumped toward battery model in the battery compartment. Heat exchange occurs in the battery compartment. Differences in temperature among inlet and exit of fluid flow (deionized water or  $\text{Al}_2\text{O}_3$ /deionized water) were measured. Details of the conditions examined in Table 1 were explained.

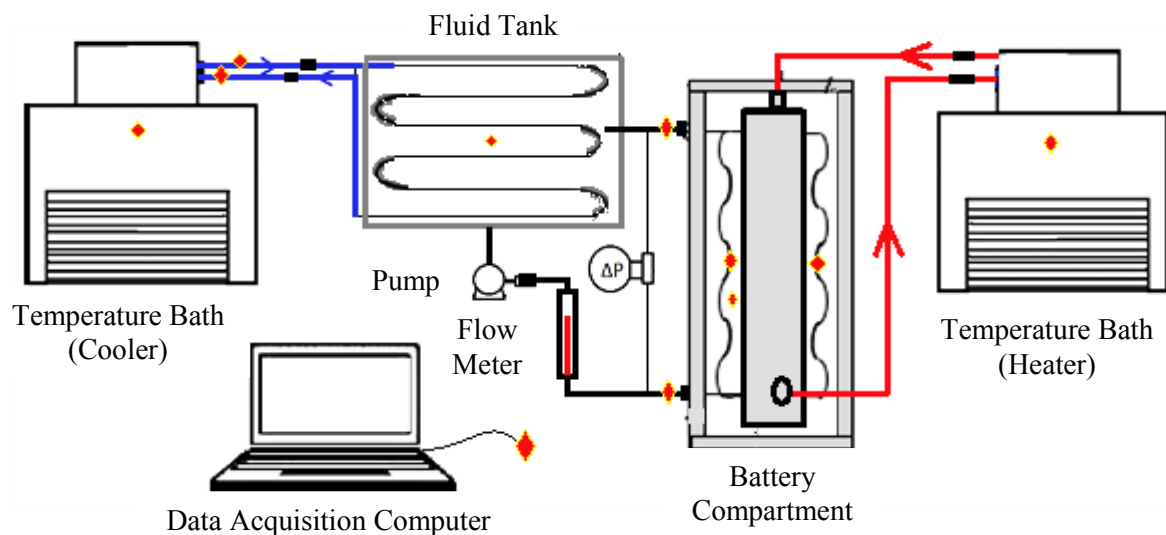


**Figure 1.** Schematic diagram for experimental setup system

A two-step method was utilized in the nanofluid preparation. Where  $\text{Al}_2\text{O}_3$  nanoparticle were dispersed in deionized water by stirring the mixture (nanofluid) for 3 hours into bottle as shown in figure 2, and after that put the bottle in ultrasonic bath used to prevent aggregation of  $\text{Al}_2\text{O}_3$  nanoparticle into deionized water for. And SDS surfactant was added to raise dispersion.



**Figure 2.** Magnetic stirring

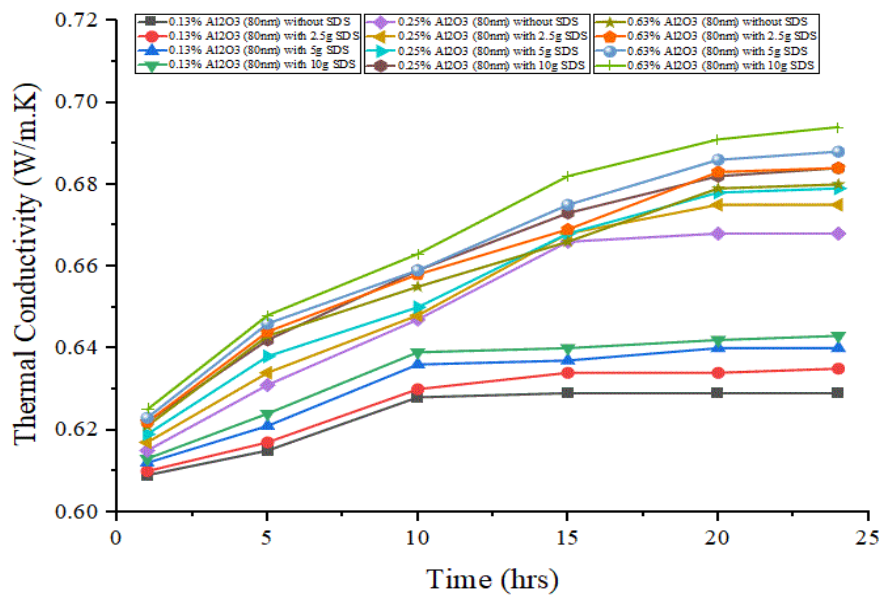


**Figure 3.** Thermal conductivity of Al<sub>2</sub>O<sub>3</sub>/deionized water nanofluids without and with SDS as a function of sonication time and various volume concentration

Figure 3 represents the sonication time impacts of nanofluid was studied at different 6 times intervals, carried out to investigate the thermal conductivity of Al<sub>2</sub>O<sub>3</sub>/deionized water nanofluids with and without surfactants (sodium dodecyl sulphate) at three various volume concentrations (0.13%, 0.25% and 0.63%) with constant temperature equal 30 °C. The values obtained were presented that the thermal conductivity of nanofluids increases with increase of sonication time and to some extent with the quantity of surfactant. Where the thermal conductivity improvement was 9% with 0.63 % volume concentration and 10 g from surfactant for Al<sub>2</sub>O<sub>3</sub> (80 nm)/deionized water nanofluid. But the difference of thermal conductivity values of Al<sub>2</sub>O<sub>3</sub>/deionized water nanofluid prepared with 1 to 10 hours of sonication time were high, while with 10 to 24 hours was low relative. It can be concluded from figure 3 that 24 hr of ultra-sonication is the best duration in the presence of a surfactant, this improvement is due to decrease of cluster sizes inside nanoparticle.

**Table 1.** Specifications and test conditions

Elements	Specifications
Volume flow rate of the pump (Q)	0.5, 0.8 and 1 L/min.
The surface area of copper tube (one coil) ( $A_{Si}$ )	0.0346 m <sup>2</sup>
Cross-sectional area of copper tube (one coil) ( $A_{ci}$ )	$1.9635 \times 10^{-5}$ m <sup>2</sup>
The ambient temperature in the compartment	40 °C
Heat load of battery model	91 W
Battery compartment size	( 0.4 × 0.31 × 0.08 ) m <sup>3</sup>

### 3. Shape and Size Nanoparticles

The morphology of the Al<sub>2</sub>O<sub>3</sub> nanoparticle was evaluated through Scanning Electron Microscope (SEM) imaging [5]. The SEM analysis is conducted to characterize the morphology as shown in figure 4, the shape of nanoparticles was semi spherical and the mean size equal  $85 \pm 5$  nm. The nanoparticles (Al<sub>2</sub>O<sub>3</sub>) was purchased from US-Research Nanomaterial.

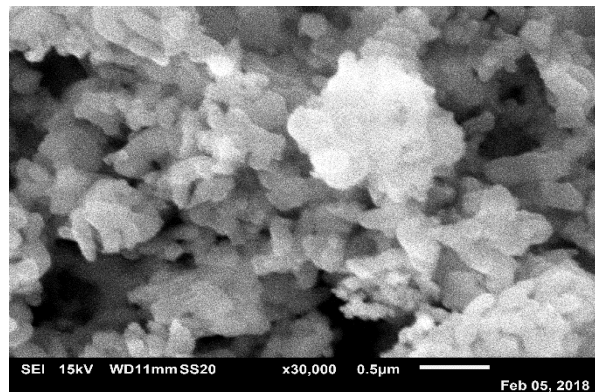


**Figure 4.** SEM image of dry  $\text{Al}_2\text{O}_3$  nanoparticles

#### 4. Experimental Apparatus

The values for thermophysical properties of the nanofluid ( $\text{Al}_2\text{O}_3$ /deionized water) at various volume concentrations are taken at the average temperature of fluid in heat exchanger.

The density of  $\text{Al}_2\text{O}_3$ /deionized water is the determined values by using Pak and Cho (1998) equation, while thermal conductivity, viscosity, and specific heat have been measured by using a KD2 Pro, viscometer (LVDV- Pro, Brookfield) and differential scanning calorimetry (DSC) respectively.

##### 4.1. Influence of surfactant and particle concentrations with various temperature on thermal conductivity

After checking the accuracy of the apparatus, the fluids were tested and thermal conductivity measured. Since nanofluid was prepared from deionized water and ( $\text{Al}_2\text{O}_3$ ) nanoparticles. The thermal conductivity of fluids was measured for the same temperature range (20 to 50 °C) at atmospheric pressure.

Figure 5 shows the change in thermal conductivity of deionized water for different temperature. This graph indicates that as the temperature increases, there is an increase in thermal conductivity. The measurement carried out two time to check from relative error for the reading, where results showed that test 2 value error less.

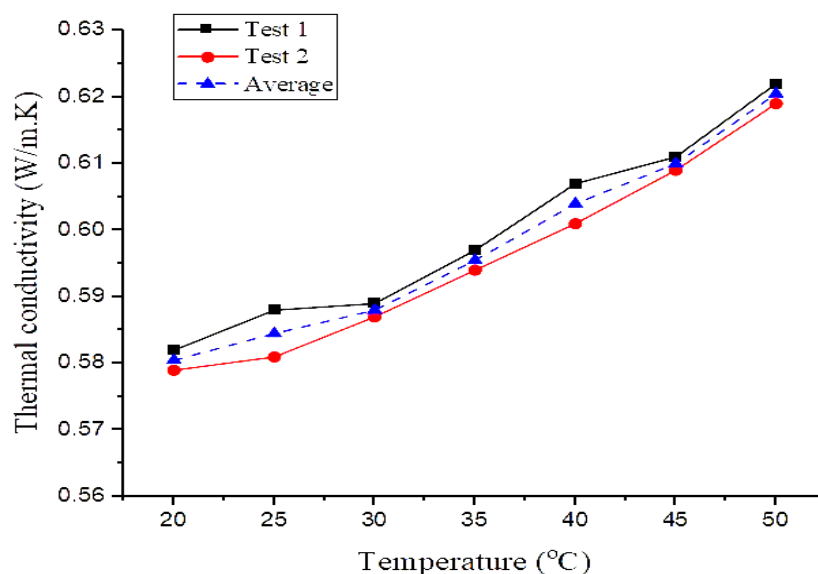


**Figure 5.** Thermal conductivity measurements for deionized water with a various temperature at atmospheric pressure

Figures from 6, 7 and 8 presents the experimental measured data change of thermal conductivity with the differences in the SDS surfactant (0g, 2.5g, 5g and 10g) and volume concentration of the  $\text{Al}_2\text{O}_3$  nanoparticles. The experiment was repeated 3 times for each sample to obtain more accurate values and the average values were taken for analysis study. The theoretical data was calculated by (Hamilton and Crosser) equation. Also show that thermal conductivity of  $\text{Al}_2\text{O}_3$ /de-ionized water increase with temperature increment.

Figures 6 (a), (b), (c) and (d) show that the thermal conductivity of  $\text{Al}_2\text{O}_3$ / de-ionized water, when volume concentration 0.13%, increases with the SDS surface a slight increase from 0 g to 10 g reach to 1%.

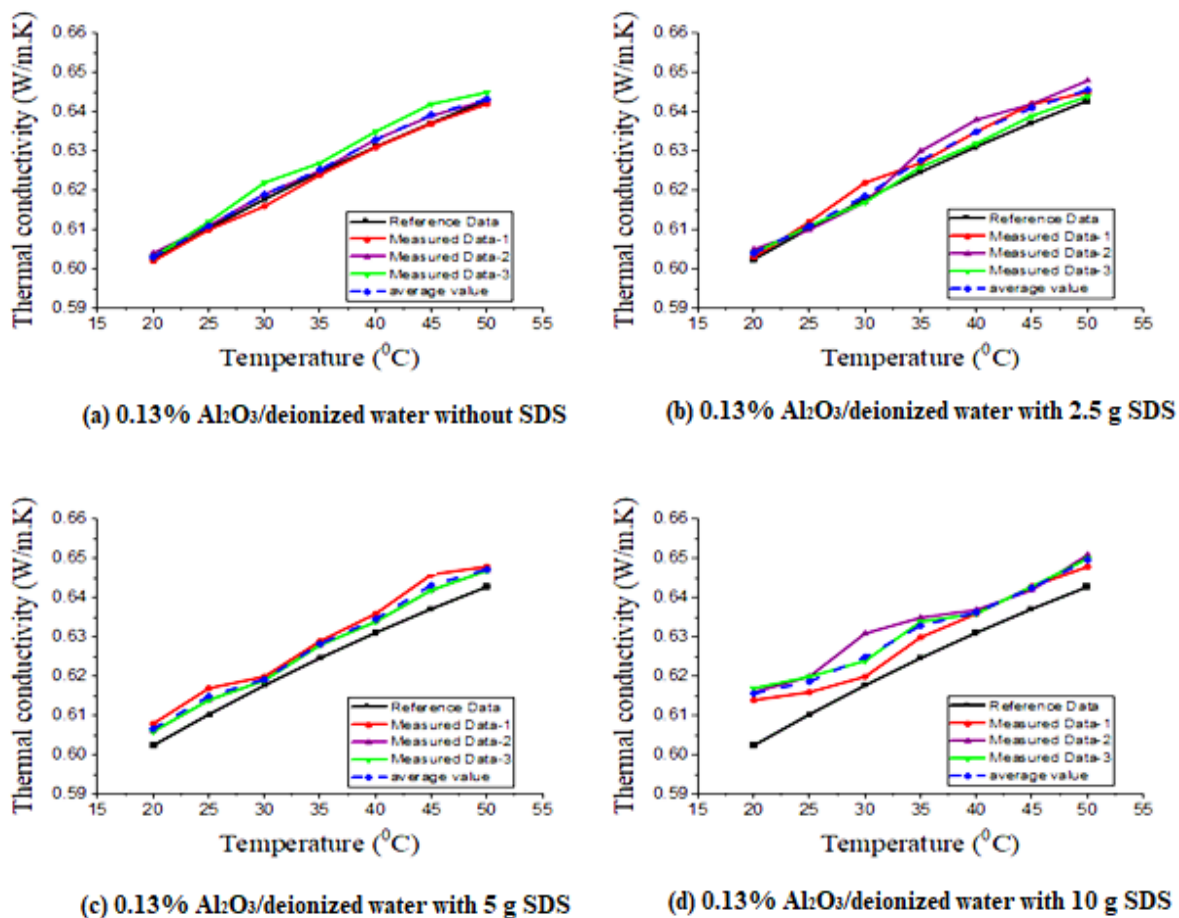
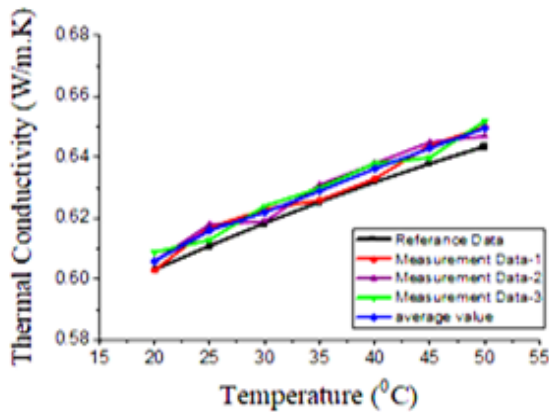
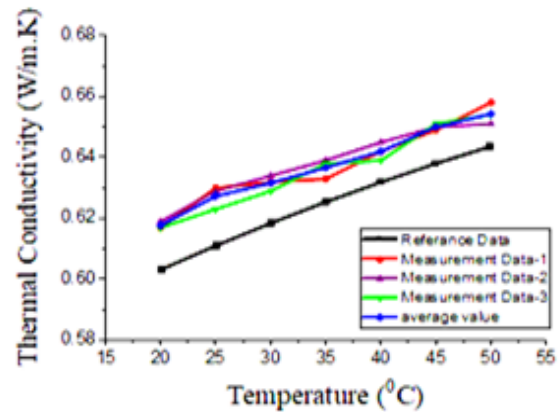


**Figure 6.** Thermal conductivity measurements for  $\text{Al}_2\text{O}_3$  (5g)/deionized water nanofluid with a various temperature at atmospheric pressure

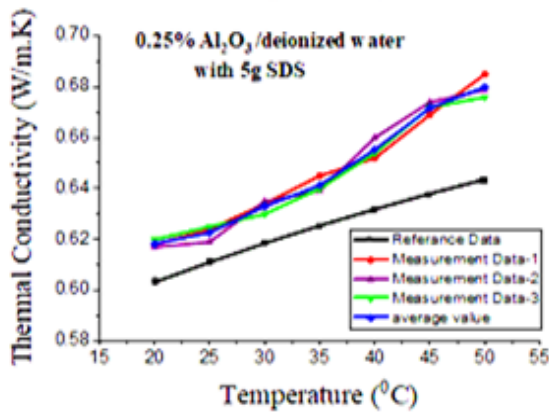
Figures 7 (a), (b), (c) and (d) show that the thermal conductivity of  $\text{Al}_2\text{O}_3$ / de-ionized water, when volume concentration 0.25%, increases with the SDS surface an increase from 0 g to 10 g reach to 5.6 %.



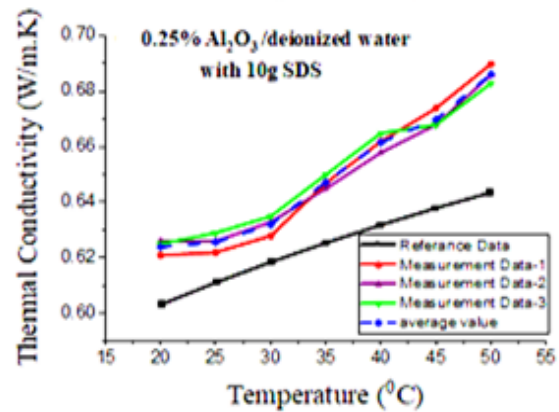
(a) 0.25% Al<sub>2</sub>O<sub>3</sub>/deionized water without SDS



(b) 0.25% Al<sub>2</sub>O<sub>3</sub>/deionized water with 2.5 g SDS

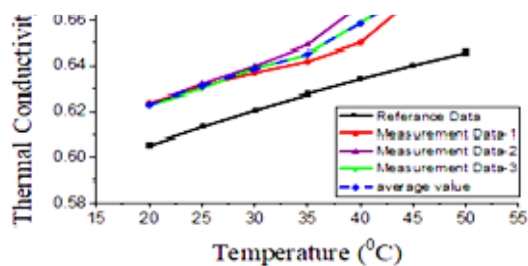


(c) 0.25% Al<sub>2</sub>O<sub>3</sub>/deionized water with 5 g SDS

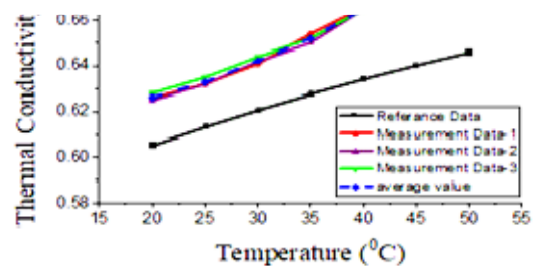


(d) 0.25% Al<sub>2</sub>O<sub>3</sub>/deionized water with 10 g SDS

**Figure 7.** Thermal conductivity measurements for Al<sub>2</sub>O<sub>3</sub> (10g)/deionized water nanofluid with a various temperature at atmospheric pressure



(c) 0.60% Al<sub>2</sub>O<sub>3</sub>/deionized water with 5 g SDS



(d) 0.60% Al<sub>2</sub>O<sub>3</sub>/deionized water with 10 g SDS

**Figure 8.** Thermal conductivity measurements for Al<sub>2</sub>O<sub>3</sub> (25g)/deionized water nanofluid with a various temperature at atmospheric pressure

#### 4.2. Influence of surfactant and particle concentrations with various temperature on viscosity

After checking the accuracy of the apparatus, the fluids were tested and dynamic viscosity measured. The dynamic viscosity of fluids was measured for the same temperature range (20 to 50 °C) with volume concentrations of 0.13, 0.25 and 0.60 vol. %. at atmospheric pressure. The experiments were conducted once per sample with a change in SDS.

Experiments displayed in figure 9 that nanofluid viscosity decreases with an increment in temperature and increase with an increasing volume concentration and SDS surfactant, and this increasing of nanofluid viscosity lead to incrementing the pressure drop, up made to consumed a larger pumping power.

Figure 9 shows that the maximum of viscosity of  $\text{Al}_2\text{O}_3$ / deionized water was decreased when increase the temperature from 20 °C to 50 °C, reach to 41.9% in case 0.13 vol. % concentration. However, there are increasing of nanofluid viscosity due to the increase the nanoparticle concentration and surfactant, reach to 41.5% in 0.60 vol. % concentration and 10g SDS surfactant.

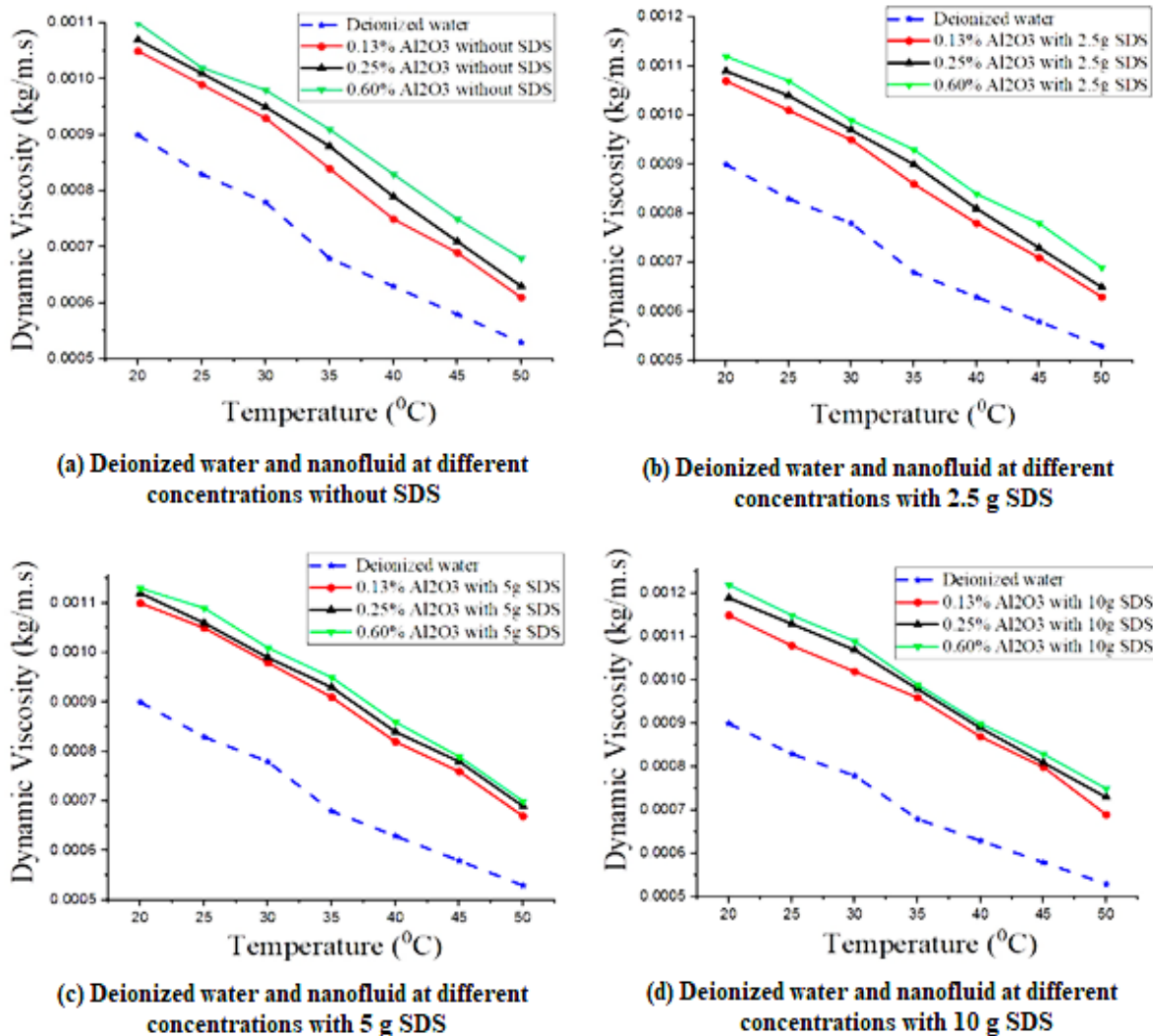


**Figure 9.** Dynamic viscosity measured for an  $\text{Al}_2\text{O}_3$ /de-ionized water nanofluid at different concentrations and temperatures with change of SDS

#### 4.3. Influence of surfactant and particle concentrations with various temperature on specific heat

After checking the accuracy of the apparatus, the fluids were tested and specific heat measured. The specific heat of fluids was measured for the same temperature range (20 to 50 °C) at atmospheric pressure.

Figure 10, it is noted that the specific heat capacity of Al<sub>2</sub>O<sub>3</sub>/ de-ionized water decreases moderately with increasing temperature to 35 °C, then there happens a slight increase to 50 °C, and decreases substantially as high nanoparticle volume concentration, reach to 1.6% in case 0.60 vol. % concentration.

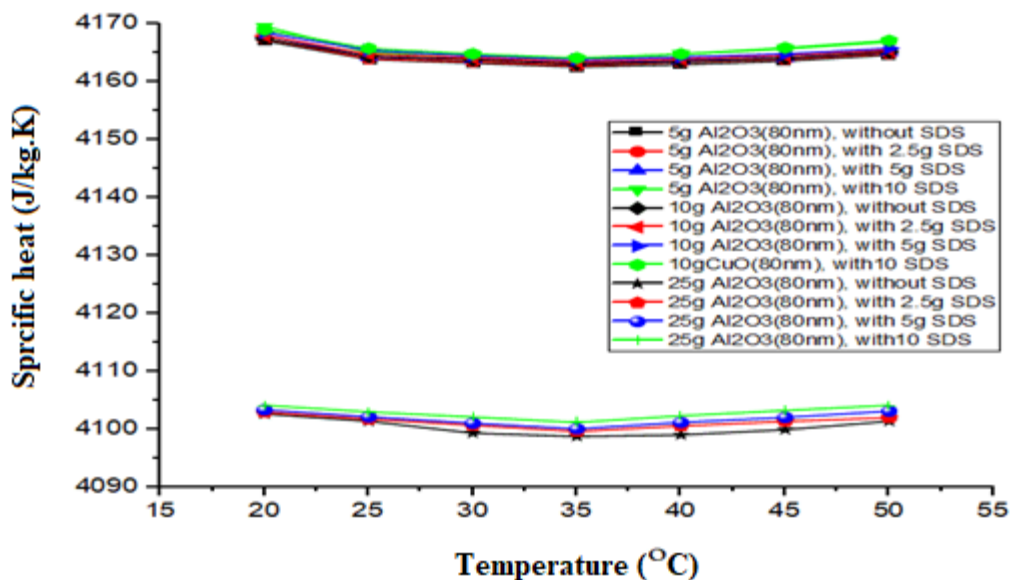


**Figure 10.** Specific heat measured for an Al<sub>2</sub>O<sub>3</sub>/deionized water nanofluid at different concentrations and temperatures with change of SDS

#### 5. Calculation of Heat Transfer Procedure

In this paper employ a forced convective heat transfer experimental to study the transportation of heat effectiveness and its influence on pressure drop of Al<sub>2</sub>O<sub>3</sub>/deionized water nanofluid. To determine the Reynolds number, Nusselt number, heat transfer coefficient and power consumption, the following procedure has been performed:

The dimensionless Reynolds number (Re) and Prandtl number are:

$$Re = \frac{\rho_f V_m d_i}{\mu_f} \quad (1)$$

$$Pr = \frac{Cp_f \times \mu_f}{K_f} \quad (2)$$

The following relation can be used to calculate the experimental Nusselt number:

$$Nu = \frac{h_{ex.} \cdot d_i}{k_f} \quad (3)$$

The heat transfer coefficient is determined by the relation [6], [7]:

$$h_{ex.} = \frac{\dot{m} Cp_f (T_{in} - T_{out})}{A_s \Delta T_{lm}} \quad (4)$$

The logarithmic mean temperature difference is calculated by the relation:

$$\Delta T_{lm} = \frac{\Delta T_h - \Delta T_c}{\ln\left(\frac{\Delta T_h}{\Delta T_c}\right)} \quad (5)$$

The formula of the peripheral area is given by

$$A_s = 2 \pi d_i L \quad (6)$$

The heat transfer rate is calculated from the following formula [8], [9]:

$$Q = \dot{m} Cp_f \Delta T = \dot{m} Cp_f (T_{out} - T_{in}) \quad (7)$$

Pressure drop throughout the heat exchanger is specified by  $\Delta p$ , which is determined by pressure differential gauge as shown in Figure 1. Now, the pumping power is calculated from the following formula [10]:

$$\text{Pumping power} = \frac{\dot{m} \times \Delta p}{\rho_f}$$

Where,  $\rho_f$  is the density of fluids,  $V_m$  is the mean velocity of fluids,  $A_c$  is cross section area of the tube,  $d_i$  is inside diameter of the tube,  $\mu_f$  is the viscosity of fluids,  $k$  is the thermal conductivity of fluids,  $T_{in}$  and  $T_{out}$  are inlet and outlet temperatures of heat exchanger,  $Cp_f$  is the specific heat of fluids,  $A_s$  is the surface area of the tubes and  $\Delta T$  is the temperature variation of the cooling fluids.

## 6. Results and Discussions

Firstly, before conducting methodical experiments on the application of Al<sub>2</sub>O<sub>3</sub>/deionized water nanofluid as fluid in the heat exchanger, some examinations were done on deionized water for check the heat exchanger and reliability of the experimental apparatus, and it comparison with Al<sub>2</sub>O<sub>3</sub>/de-ionized water nanofluid. The results of the experiments were obtained at constant inlet temperature of  $20 \pm 0.5^\circ\text{C}$ .

Table 2, show the thermophysical properties measurement results after the preparation of the nanofluid directly. And noted that 0.13 vol. %, 0.25 vol. % and 0.60 vol. % with 10 g SDS surfactant were more stable, so will be done examinations on these concentrations only with 10 g SDS surfactant.

**Table 2.** Summary of thermophysical properties of fluids at bulk mean temperature with change concentrations and surfactant

Thermophysical properties	Volume concentration (%)	SDS Surfactant (g)	Results	Notes
Thermal conductivity (W/m.K)	0	0	0.579	It is low of de-ionized water
	0.13	0	0.603	Increases with the raise of nanoparticle volume concentration, SDS surfactant and temperature.
		2.5	0.604	
		5	0.60667	
		10	0.61567	
	0.25	0	0.606	
		2.5	0.61767	
		5	0.61833	
		10	0.624	
	0.60	0	0.61167	
		2.5	0.62	
		5	0.6233	
10		0.62633		
Viscosity (kg/m.s)	0	0	0.0009	It is low of de-ionized water
	0.13	0	0.00105	Increases with the raise of nanoparticle volume concentration, SDS surfactant and decreasing with raise of temperature.
		2.5	0.00107	
		5	0.0011	
		10	0.00115	
	0.25	0	0.00107	
		2.5	0.00109	
		5	0.00112	
		10	0.00119	
	0.60	0	0.0011	
		2.5	0.00112	
		5	0.00113	
10		0.00122		
Specific heat (J/kg K)	0	0	4183	It is high of de-ionized water
	0.13	0	4167.07	There is a slight increase with the raise of SDS surfactant and significant decrease with high concentrations of nanofluid in deionized water.
		2.5	4167.44	
		5	4168.05	
		10	4169.61	
	0.25	0	4167.48	
		2.5	4167.98	
		5	4168.51	
		10	4168.99	
	0.60	0	4102.68	
		2.5	4102.98	
		5	4103.38	
10		4104.18		

**Table 3.** Summary of results ( $\text{Al}_2\text{O}_3$ / de-ionized water) at bulk mean temperature with change concentrations and surfactant

Mass flow rate L/min	Volume Concentrations	SDS Surfactant	Reynolds number	Prandtl number	Heat transfer rate (Q) W
0.5	0 %		1178.65	7.33	53.5
	0.13%	5	966.882	7.57	72.4
		10	924.844	7.85	73.1
	0.25%	5	953.144	7.65	77.2
		10	897.077	8.1	77.6
	0.60%	5	955.146	7.53	87.8
10		884.685	8.1	88.3	
0.8	0%		1885.85	7.33	85.5
	0.13%	5	1547.01	7.57	115.8
		10	1479.75	7.85	117
	0.25%	5	1525.03	7.65	123.5
		10	1435.323	8.1	124.1
	0.60%	5	1528.234	7.53	140.5
10		1415.496	8.1	141.3	
<b>1</b>	0%		2357.31	7.33	106.9
	0.13%	5	1933.76	7.57	144.8
		10	1849.69	7.85	146.2
	0.25%	5	1906.288	7.65	154.4
		10	1794.154	8.1	155.1
	0.60%	5	1910.293	7.53	175.6
10		1769.369	8.1	176.6	

Experimental results showed in table 3 that the Reynolds number decremented with increasing volume concentration of nanoparticles and the SDS surfactant, and it was observed that Prandtl number increased with both increase of volume concentration and surfactant and not change with rising flow rate. And dispersion nanoparticles, Reynolds number and SDS surfactant on thermal small areas were investigated. Furthermore, the influence of flow laminar on the heat transfer rate was studied. Found that the heat transfer rate was incremented with rising flow rate, volume concentration of nanoparticle, SDS surfactant, and Reynolds number.

## 7. Conclusions

In this article, the heat transfer rate of fluids in the simulated battery cooling system (heat exchanger) has been measured experimentally. The fluids are base fluid (de-ionized water) and nanofluid ( $\text{Al}_2\text{O}_3$ /de-ionized water) at different volume concentrations without and with surfactants. The results are concluded as follows:

- The influence of ultra-sonication time where it was improved slowly for thermal conductivity and stability, due to used indirect ultra-sonic.
- It was observed that the nanofluid at the concentrations of 0.13 vol.% and 0.25 vol.%, had stabilized for two months after preparation when adding the 10g from SDS surfactant. While 0.60 vol.% had stabilized for 5 weeks with same SDS surfactant.
- The thermal conductivity values of nanofluids were found to be increased with increasing temperature and increasing with rising of volume concentration nanoparticles and surfactant.

- The viscosity values of nanofluids were found to be decreased with increasing temperature and increasing with rising of volume concentration nanoparticles.
- The specific heat values of nanofluids were found to be decreased with increasing temperature to certain point, and then rises slowly. And also, specific heat values of nanofluids slightly decreasing with small concentration nanoparticles and surfactant, while clearly decreasing with high concentration.
- Experimentally, it was observed that heat source (battery model) equal 91 W, when using the deionized water at 1 l/min flow rate gives improvement by 17.5%, while using Al<sub>2</sub>O<sub>3</sub>/de-ionized water nanofluid at same flow rate and 0.60% vol.% concentration with 10 g SDS surfactant gives improvement by 94%. This means that Al<sub>2</sub>O<sub>3</sub>/de-ionized water nanofluid gives better improvement than deionized water by 65%.

## References

- [1] I. Manna, "Synthesis, characterization and application of nanofluid - An overview," *Journal of the Indian Institute of Science*, vol. 89, no. 1, pp. 21–33, 2009.
- [2] N. A. Bin-Abdun, Z. M. Razlan, A. B. Shahrman, K. Wan, D. Hazry, S. Faiz Ahmed, N. H. Adnan, R. Heng, H. Kamarudin, and I. Zunaidi, "Base fluid in improving heat transfer for EV car battery," in *AIP Conference Proceedings*, 2015, vol. 1660.
- [3] X. Wang, X. Xu, and S. U. S. Choi, "Thermal Conductivity of Nanoparticle - Fluid Mixture," *Journal of Thermophysics and Heat Transfer*, vol. 13, no. 4, pp. 474–480, 1999.
- [4] I. M. Shahrul, I. M. Mahbulul, R. Saidur, and M. F. M. Sabri, "Experimental investigation on Al<sub>2</sub>O<sub>3</sub>-W, SiO<sub>2</sub>-W and ZnO-W nanofluids and their application in a shell and tube heat exchanger," *International Journal of Heat and Mass Transfer*, vol. 97, pp. 547–558, 2016.
- [5] Babita, S. K. Sharma, and G. S. Mital, "Preparation and evaluation of stable nanofluids for heat transfer application: A review," *Experimental Thermal and Fluid Science*, vol. 79, pp. 202–212, 2016.
- [6] K. Y. Leong, R. Saidur, M. Khairulmaini, Z. Michael, and A. Kamyar, "Heat transfer and entropy analysis of three different types of heat exchangers operated with nano fluids ☆," vol. 39, pp. 838–843, 2012.
- [7] C. J. Ho and W. C. Chen, "An experimental study on thermal performance of Al<sub>2</sub>O<sub>3</sub> / water nano fluid in a minichannel heat sink," vol. 50, pp. 516–522, 2013.
- [8] T. L. Bergman, F. P. Incropera, D. P. DeWitt, and A. S. Lavine, *Fundamentals of heat and mass transfer*. John Wiley & Sons, 2011.
- [9] R. S. Vajjha, D. K. Das, and D. P. Kulkarni, "International Journal of Heat and Mass Transfer Development of new correlations for convective heat transfer and friction factor in turbulent regime for nanofluids," *International Journal of Heat and Mass Transfer*, vol. 53, no. 21–22, pp. 4607–4618, 2010.
- [10] P. Taylor, M. Kahani, S. Z. Heris, and S. M. Mousavi, "Journal of Dispersion Science and Technology Effects of Curvature Ratio and Coil Pitch Spacing on Heat Transfer Performance of Al<sub>2</sub>O<sub>3</sub> / Water Nanofluid Laminar Flow through Helical Coils Effects of Curvature Ratio and Coil Pitch Spacing on Heat Transfer," no. November 2014, pp. 37–41, 2013.

## Acknowledgments

The authors fully acknowledged Universiti Perlis Malaysia for the support which makes this important research viable and effective.